

A Physically-Based Abrasive Wear Model for Composite Materials

Gun Y. Lee^{1,3}, C. K. H. Dharan¹, and R. O. Ritchie^{2,3}

¹*Department of Mechanical Engineering, University of California, Berkeley, CA 94720 -1750*

²*Department of Materials Science & Engineering, University of California, Berkeley, CA 94720-1760*

³*Materials Sciences Division, Lawrence Berkeley National Laboratory, Berkeley, CA 94720*

SUMMARY: A simple physically-based model for the abrasive wear of composite materials is presented based on the mechanics and mechanisms associated with sliding wear in soft (ductile) matrix composites containing hard (brittle) reinforcement particles. The model is based on the assumption that any portion of the reinforcement that is removed as wear debris cannot contribute to the wear resistance of the matrix material. The size of this non-contributing portion of reinforcement is estimated by modeling three primary wear mechanisms, specifically, plowing, cracking at the matrix/reinforcement interface or in the reinforcement, and particle removal. Critical variables describing the role of the reinforcement, such as relative size, fracture toughness and the nature of the matrix/reinforcement interface, are characterized by a single contribution coefficient, C . Predictions are compared with the results of experimental two-body (pin-on-drum) abrasive wear tests performed on a model aluminum particulate-reinforced epoxy-matrix composite material.

KEYWORDS : Composites, abrasive wear, fracture toughness, reinforcement size

INTRODUCTION

As advanced engineering materials, composites are used in many applications where high wear resistance is required; these include electrical contact brushes, cylinder liners, artificial joints, and helicopter blades. Indeed, compared to monolithic materials, wear resistance can generally be enhanced by introducing a secondary phase(s) into the matrix material [1-6]. In this fashion, the wear properties can be varied substantially through changes in the microstructure, the morphology, volume fraction and mechanical properties of the reinforcing phase, and the nature of the interface between matrix and reinforcement.

In order to obtain optimal wear properties without compromising the beneficial properties of the matrix material, an accurate prediction of the wear of composites is essential. Unfortunately, for abrasive wear, existing models for composites are highly simplified and do not readily predict the role of the composite microstructure. In general, they are based on two simplified equations, the first of which, the inverse rule of mixtures, was introduced for two-phase composites by Khrushchov [7]:

$$\frac{1}{W_C} = \frac{V_{M1}}{W_{M1}} + \frac{V_{M2}}{W_{M2}}, \quad (1)$$

where W and V are, respectively, the wear rates and volume fractions of the matrix (designated by subscript $M1$) and reinforcement (designated by $M2$). Note that the wear resistance, R , in Khruschov's original formulation is given by the reciprocal of the wear rate, $R = 1/W$.

Eq. (1) is based on the assumption that the components of the composite wear at an equal rate. Consequently, Khruschov's equation predicts that the abrasive wear resistance is linearly additive and that the wear resistance of the composite is simply the sum of the products of wear resistance and volume fraction for each component. Eq. (1) for a two-phase composite is plotted in Fig. 1. Since the wear rate of the harder reinforcement is typically much smaller than that of the matrix, this relationship predicts that the abrasive wear behavior of a composite will be governed primarily by the reinforcement.

The second wear equation for multiphase materials, introduced by Zum-Gahr to explain experimental data, is the linear rule of mixtures; here, the wear behavior of a composite is not dominated by a single phase [6]. Instead, the contribution from each component is linearly proportional to its volume fraction in the composite:

$$W_C = V_{M1} \cdot W_{M1} + V_{M2} \cdot W_{M2}, \quad (2)$$

and is also plotted in Fig. 1. In this model, the abrasive wear rate of the composite decreases linearly with increasing volume fraction of reinforcement. This expression was also derived by Axen and Jacobson using the equal pressure assumption that all components of a composite carry the same specific load [8]. A cyclic wear model for oriented fiber composites that predicted narrower bounds for abrasive wear behavior was proposed by Yen and Dharan [9]. In their paper, fiber instability due to preferential wear of the softer matrix resulted in cyclic generation of wear debris during the wear process. However, interface toughness and other physically-based factors were not considered in their model.

While Eqs. (1) and (2) are presumed to provide upper and lower limits for abrasive wear rates in a composite, this is not confirmed by some experimental results due to the simplified, non-physically based nature of the two models. Indeed, this can be appreciated in Fig. 1, which shows experimental results for composites that are reinforced with hard particles [1,10-14]. Both models rely on the notion that all components in the composite wear in the same way as they would in a bulk material; consequently, the contribution of each component can depend only on its volume fraction and wear rate. The effects of other important factors, such as interfacial properties between the distinctive phases, relative sizes, and the fracture toughness of these phases, are not considered, even though it is clear that they have a significant influence on abrasion in composites [1,5,15-21]. Specifically, the wear rates of composites can exceed the upper bound given by Eq. (2) in that they are higher than that of the pure matrix material [1,10-

14]; this implies that the presence of reinforcement enhances the wear rate instead of reducing it – the negative reinforcement effect. Experimental data showing the negative reinforcement fall in the area denoted by region A in Fig. 1. The inability to predict such effects represents a major limitation of existing abrasive wear models for composite materials.

In the present study, a new physically-based abrasive wear model for composite materials with hard reinforcements is developed based on three primary wear mechanisms: plowing, cracking at the interface or in the reinforcement, and particle removal. The effects of critical factors, such as, interfacial properties, and geometrical and mechanical properties of the reinforcement, are specifically considered. The model introduces a factor related to the fracture toughness of the matrix/reinforcement interface and the reinforcement, and the relative size of the reinforcement relative to the abrasive grains. It predicts the negative reinforcement effect and is useful for interpreting wear data in terms of the role of the interface and reinforcement size. The model may also assist in the design of abrasive wear-resistant composite materials. The predictions of the proposed model are verified by experimental abrasive wear studies conducted on a model aluminum particulate-reinforced epoxy matrix composite.

DUCTILE- AND BRITTLE-MATRIX COMPOSITES

The sliding of abrasives on a solid surface results in volume removal. The mechanism of wear depends on the mechanical properties of the solid [22,23]. In a ductile solid, the primary wear mechanism is related to plastic deformation; correspondingly, the hardness of the material is a key parameter in governing the amount of material removal. However, the dominant mechanism in a brittle solid depends on fracture at, or near, the surface such that the governing property is the toughness of the material.

To improve wear resistance, additional phase(s) can be introduced to either a ductile or a brittle matrix material. However, the required mechanical properties of the reinforcement and the role of the reinforcement will be different in ductile vs. brittle matrices. For a ductile matrix, a hard secondary phase is needed to reduce wear, such that the presence of the hard reinforcement increases the effective hardness of the matrix, thereby reducing the penetration of the abrasive medium. Consequently, increasing the effective hardness acts to reduce the amount of material removed. Here, we term such a multiphase system composed of a ductile matrix and a hard reinforcement as a hard-reinforcement or *hardened composite*. On the other hand, a tough reinforcement phase is needed for a brittle matrix to increase wear resistance. The presence of a tough secondary phase reduces the tendency for fracture at, or near, the surface, and therefore tends to decrease the wear rate. In certain ceramic-matrix composites, i.e., brittle matrix materials, the addition of a relatively ductile second phase can result in synergistically favorable wear behavior in which the composite wear rate can be less than the wear rates of the individual constituents. This behavior is denoted by region B in Fig. 1 and has been observed in ceramic composites [2,3]. A multiphase system composed of a brittle

matrix and a tough reinforcement may be termed a ductile-reinforcement or *toughened composite*.

The present study is focused on hard-reinforcement particulate composites, which have been the object of most modeling studies of the wear of composites in the past (e.g., [6,7]). We will consider reinforcement volume fractions in the range 0 to 0.5, since at higher volume fractions one can expect significant particle-particle interactions. Moreover, from a practical standpoint, it is difficult to manufacture particulate composites at volume fractions greater than 0.5 due to void formation resulting from imperfect wetting and agglomeration.

ABRASIVE WEAR MODEL

A model is developed with simplified geometry in two dimensions, namely a triangular abrasive medium particle acting on a composite containing idealized rectangular reinforcements. The model is based on the “equal wear rate assumption”; this postulates that the different components of a composite wear at steady state at an equal rate through the redistribution of the specific loads [7,8,24]. A general schematic drawing of a two-phase composite with a ductile matrix and a hard reinforcement in abrasion is shown in Fig. 2. The characteristic size of the reinforcement is represented by the parameter D_R .

If the fracture toughness of the matrix/reinforcement interface exceeds the minimum toughness of either constituent (a “strong” interface) and the fracture in the reinforcement is not favorable, then plowing will be the predominant wear mechanism; consequently, the resulting wear debris will be small in relation to the reinforcement size. With such a strong interfacial bonding and a tough reinforcing phase, the entire reinforcement particle will contribute to improving wear resistance. Both rules of mixtures, Eqs. (1) and (2), are commonly based on this assumption.

In practice, however, the reinforcement is removed due to failure at the matrix/reinforcement interface or in the reinforcement. The interfacial bonding between constituent materials may not be strong due to chemical incompatibility, mismatch in thermal expansion and elastic properties, e.g., stiffness, at the interface [25], and the presence of impurities and/or voids that arise during fabrication. In this case, the motion of the abrasive medium induces interfacial failure and debonding around the reinforcing particles. On the other hand, if the matrix/reinforcement interface provides a strong bond and the reinforcing phase has a low resistance to fracture, failure can occur in the reinforcement, which is often observed in composites under severe wear conditions [19-21].

Since the portion of the reinforcement that is removed due to failure at the interface or in the reinforcement cannot further contribute to improving wear properties of the matrix, its contribution to the wear resistance is inversely proportional to its relative size. The size of this non-contributing portion (NCP) can be estimated by modeling the three

primary abrasive wear mechanisms, namely plowing, cracking at the interface or in the reinforcement, and particle removal. Based on this information, a new relationship for the abrasive wear rate of a composite is developed.

A. *Plowing mechanism*

The depth of penetration, x , of the abrasive medium depends on its geometry, the applied normal load, and the mechanical properties of a composite (relative to the abrasive medium). While the abrasive medium is moving, contact with the substrate occurs only over its half-front surface. Under an indentation load L , the depth of penetration of the abrasive particle can be written as:

$$L = \frac{1}{2}(2w \cdot b \cdot H_C) \text{ and } \frac{x}{w} = \tan \mathbf{q} \text{ ,}$$

$$x = \frac{L}{b \cdot H_C} \tan \mathbf{q} \text{ ,} \quad (3)$$

where b is the thickness of the substrate and abrasive medium, and H_C is the hardness of the composite. The magnitude of plowing load F_p required to plastically deform and remove material is proportional to the depth of penetration of the abrasive medium. The abrasive medium will plow the matrix and the reinforcement alternatively, and experience different plowing loads for the different phases (Fig. 3). The expression for the plowing load on each phase can be expressed by employing the indentation load approximation:

$$F_p = x \cdot b \cdot H_i \text{ ,} \quad (4)$$

where H_i is the hardness of either the matrix or reinforcement material.

If the spacing, d , between individual abrasive particles is small compared to the extent of their respective stress fields, then an interaction between neighboring stress fields will occur (Fig 3). Consequently, stresses around each abrasive particle will depend on the average distance between these particles and the magnitude of the plowing loads.

B. *Cracking mechanisms*

In a hardened composite composed of a ductile (soft) matrix and a hard (brittle) reinforcement, a maximum load is applied on the system when the abrasive medium plows the reinforcing phase, $F_p = (F_p)_R$ in Eq. (4). Its magnitude depends on the depth of penetration, x , the average spacing between abrasive particles, d , and the hardness of the reinforcement, H_R . If the values of these parameters are very small compared to the size of the reinforcement, plowing is the dominant material removal mechanism. However, when their values become comparable or larger than that of the reinforcement, material may be removed due to the failure/cracking at the matrix/reinforcement interface or in the

reinforcing phase (Fig. 4). The trajectory of the crack depends on the relative toughness of the interface to that of the reinforcing material.

a. Cracking at the matrix/reinforcement interface

When the ratio of the fracture toughness of the interface, G_{if} , and the reinforcing material, G_R , is less than approximately 0.25 for this geometry (this ratio does vary with the orientation of the crack [26]), plowing by the abrasive medium can lead to the propagation of a crack in the “weak” interface. (Fig. 4(a)), i.e., when [26]:

$$\frac{G_{if}}{G_R} < \frac{1}{4}. \quad (5)$$

b. Cracking in the reinforcement

On the other hand, if the interfacial bonding between the matrix and the reinforcement is good (a “strong” interface), the crack will propagate into the reinforcing phase (Fig. 4(b)). In this case, the ratio of the interfacial fracture toughness to that of the reinforcing phase must be higher than 0.25 (for a crack normal to the interface):

$$\frac{G_{if}}{G_R} \geq \frac{1}{4}. \quad (6)$$

The lengths of the interfacial crack, a_{int} , and the crack in the reinforcement, a_R , depend on the fracture toughness and parameters such as the average distance, d , between abrasive the medium and the plowing loads, viz:

$$\text{crack size} = f\{G_i, (F_P)_R, d, (F_P)_{n+1}\}, \quad (7)$$

where G_i represents either the interfacial fracture toughness, G_{if} , for the case of an interfacial crack of length a_{int} , or the fracture toughness of the reinforcing material, G_R , for a crack of length a_R in the reinforcement.

C. Particle removal

In a hardened composite system with a weak interface, continuous plowing of the abrasive medium reduces the level of the wear surface until the tip of the interfacial crack finally reaches the bottom of the reinforcement. The plowing of the next abrasive medium will cause further propagation of the interfacial crack around the reinforcing particle (Fig. 5(a)). The continuous motion of the abrasive medium can result in complete removal of the remaining portion of the reinforcement leaving a void of the same size on the surface. As a portion of reinforcement is now removed as a large mass (due to interfacial failure), it cannot contribute to the wear resistance. It is assumed that the size of the crack, a_{int} at the interface or a_R in the reinforcement, of a composite under

given wear conditions is constant. The fraction of this “non-contributing portion (NCP)” is:

$$\text{NCP} = \frac{(x + a_{\text{int}})}{D_R} \quad (\text{crack at interface}) , \quad (8)$$

where x is the depth of penetration of the abrasive medium, a_{int} is the size of the interfacial crack, and D_R is the size of the reinforcement (Fig. 5(b)).

However, with a relatively strong interface, plowing of the abrasive medium will lead to crack growth in the reinforcement (Fig. 4(b)). It is assumed that the crack, a_R , propagates parallel to the wear surface. While the abrasive medium is moving through the reinforcing phase, the crack, a_R , stays in front of it. When the tip of the crack reaches the reinforcement/matrix interface, further motion of the abrasive medium will cause removal of a portion of the reinforcement as a wear particle (Fig. 6(a)). As the size of this non-contributing portion (NCP) with respect to the path of abrasive medium is the product of the depth of penetration, x , and the size of crack, a_R , as shown in Fig. 6(b), the fraction of the non-contribution portion of the reinforcement can be estimated by:

$$\text{NCP} = \frac{x \cdot a_R \cdot N}{D_R^2} = \frac{a_R}{D_R} \quad (\text{crack in reinforcement}) , \quad (9)$$

where a_R is the size of the crack in the reinforcement, x is the depth of penetration of the abrasive medium, and D_R is the size of the reinforcement.

In terms of these three primary wear mechanisms, the wear behavior of a two-phase composite is akin to that of a three-phase composite composed of a matrix, reinforcement and pores. The volume fraction of the porous section is equal to the volume fraction of the non-contribution portion of the reinforcement, which is the product of volume fraction of reinforcement V_R and the fraction of the non-contributing portion (Eq. (10)):

$$\begin{aligned} V_{\text{pore}} &= V_R \cdot \left(\frac{(x + a_{\text{int}})}{D_R} \right) \quad (\text{crack at interface}) , \\ V_{\text{pore}} &= V_R \cdot \left(\frac{a_R}{D_R} \right) \quad (\text{crack in reinforcement}) . \quad V_R \leq 0.5 \quad (10) \end{aligned}$$

Thus, the net volume fraction of the reinforcement, which contributes to the wear resistance, can be written as:

$$V_{\text{net}} = V_R - V_{\text{pore}} . \quad V_R \leq 0.5 \quad (11)$$

The wear rate of the three-phase composite can again be obtained based on the “equal wear rate assumption”:

$$\frac{1}{W_C} = \frac{V_m}{W_m} + C \cdot \frac{V_R}{W_R} + (1-C) \cdot \frac{V_R}{W_{pore}} \quad , \quad V_R \leq 0.5 \quad (12)$$

where W_C , W_m , W_R and W_{pore} are the wear rates of composite, matrix, reinforcement and pores, V_m and V_R are the volume fractions of the matrix and the reinforcement, and C is a new parameter, which we term the *contribution coefficient* of the reinforcement. This parameter describes the relative contribution of each of the primary wear mechanisms and is defined as:

$$C = \left(1 - \frac{(x + a_{int})}{D_R} \right) \quad (\text{crack at interface}) \quad ,$$

$$C = \left(1 - \frac{a_R}{D_R} \right) \quad (\text{crack in reinforcement}) \quad . \quad (13)$$

Since the third term on the right side of Eq. (12) will vanish because the wear resistance of pores is equal to zero, $1/W_{pore} = 0$, we can obtain a final expression for the abrasive wear rate of a composite from this physically-based mechanistic model as:

$$\frac{1}{W_C} = \frac{V_m}{W_m} + C \cdot \frac{V_R}{W_R} \quad . \quad V_R \leq 0.5 \quad (14)$$

The contribution coefficient parameter, C , represents the effects of critical factors, including the fracture toughness and the relative size of the reinforcement; its magnitude varies from zero to unity.

EXPERIMENTS

A. Materials

To provide some degree of experimental verification of the proposed model, abrasive wear tests were conducted with a model composite system involving an epoxy matrix with spherical aluminum alloy particulate reinforcement. In order to minimize the effect of the mismatch in coefficient of thermal expansion, a room temperature curing epoxy was selected as the matrix material; this was DER 331 epoxy resin and DEH 24 hardener from Dow Chemical, Midland, MI USA. The epoxy was reinforced with 6061 aluminum metal particles provided by Valimet Inc., Stockton, CA USA; the particles were nominally spherical with an average size of $\sim 100 \mu\text{m}$ (Fig. 7).

In order to vary the contribution coefficient C in Eq. (14), tests were performed on composites with different matrix/reinforcement interfacial toughnesses and with different relative sizes of reinforcement. A “strong” interface was achieved by reinforcing the epoxy with uncontaminated particles, whereas a “weak” interface was achieved by prior coating of the particles with a thin layer of silicone. The relative sizes of the

reinforcement were varied by conducting tests on different abrasive sizes (35 ~ 326 μm), as shown in Fig. 8.

Tests were performed for specimens containing 0, 20, 40 and 100 percent by volume of reinforcement. The composites were fabricated by vacuum stir-casting. This process consists of mixing metal particles in a catalyzed liquid epoxy followed by casting in an open mold (9.5 mm diameter and 20 mm length) in a vacuum. The mixture was cured for 7 days at room temperature.

B. Abrasive wear test

Two-body abrasive wear tests were conducted on a pin-on-drum abrasive wear tester, designed for standard wear tests described in ASTM Standard D5963-97a. In this method, the test specimen translates over the surface of an abrasive paper, which is mounted on a revolving drum, with the resulting wear of the material expressed as volume loss [27]. The test setup is schematically illustrated in Fig. 9.

An alumina (Al_2O_3) abrasive which is substantially harder than either the matrix or the reinforcement was used. The pin specimen, 0.95 mm in diameter and 20 mm long, was placed on the top of the drum, which was then rotated at a fixed angular speed of 25 RPM; this gives a tangential velocity at the contact surface of 0.2 m/s. While the drum was rotating, the specimen is translated at the speed of 4.2 mm/rev along the axis of rotation. Thus, the specimen is continuously in contact with new abrasive surface. A static normal load, L , was applied directly on the specimen to press it against the center of the drum (Fig. 9); its magnitude was varied from 1 to 5 N, corresponding to a normal stress ranging from ~14 to 69 kPa. Throughout the test, the sliding distance was fixed at 39.2 m (80 revolutions). Table 1 shows roughness and typical groove depths in the neat resin for the abrasive sizes used in the experiments. Peak-to-valley distances ranged from 5 to 90 μm and were measured using a Talysurf 10 profilometer. All tests were carried out in dry ambient air laboratory conditions.

RESULTS AND DISCUSSION

A. Model Predictions

Predicted wear rates from Eq. (14) for the two ideal composites with different contribution coefficients and volume fractions are shown in Fig. 10. The two composites, termed composite 1 and 2, differ in their relative wear resistance; the abrasive wear resistance of the reinforcement in composite 2 is twice as large as that of the reinforcement in composite 1.

From Fig. 10, predictions of the wear rates of the composites at a fixed volume fraction can be obtained. These wear rates depend strongly on the contribution coefficient, C , of the reinforcement. When $C = 1$, i.e., in the absence of particle removal such that the reinforcement wears in the same way as if it were in bulk, the size of the

non-contributing portion of the reinforcement, $(x + a_{\text{int}})$ in Fig. 5 (b) and a_R in Fig. 6(b), becomes small compared to the total size of the reinforcement D_R . Under these conditions, the model predicts wear rates that are equal to the lower limit of the inverse law of mixtures model (Eq. (1)). As the contribution coefficient is reduced, wear rates are predicted to increase above this lower limit. Indeed, as $C \rightarrow 0$, predicted wear rates of the composites become higher than that of the matrix, demonstrating the negative reinforcement effect.

The value of C depends strongly on the penetration of the abrasive medium, x , and the interfacial crack size, a_{int} . Thus for the case of interfacial cracking, the toughness of the matrix/reinforcement interface is a crucial factor governing the magnitude of a_{int} . If the interfacial toughness is reduced, the size of the interfacial crack increases and thus the value of C is decreased. Consequently, the model predicts that the wear rate of the composite will be increased by any reduction in the interfacial toughness. A corresponding increase in the depth of penetration will effectively reduce the relative size of the reinforcement. This lowers the value of C and consequently increases the wear rate of the composite. In contrast, raising the interfacial toughness and decreasing the depth of penetration will enhance the contribution of the reinforcement and thus reduce the wear rate of the composite. Similar features will be observed in the case of reinforcement fracture as well because the contribution coefficient C is also a function of the factors governing the crack size, a_R . The fracture toughness of the reinforcement and the depth of penetration are primary factors. Thus, raising the fracture toughness of reinforcing material and reducing the depth of penetration, x , will increase the contribution coefficient, and vice versa.

Another notable observation from these predictions is that even though composite 2 has a more wear-resistant reinforcement, the overall wear resistance of the composite depends also on factors such as the toughness and relative reinforcement size, i.e., on the value of C . Thus, the present model highlights the fact that choosing a reinforcement solely on its bulk wear resistance without consideration of these other factors will not guarantee the optimal wear characteristics of the composite itself. For example, at a reinforcement volume fraction, $V_R = 0.5$, the critical value of C below which the wear rate exceeds the upper bound is about $C = 0.28$ in the composite with the more wear-resistant reinforcement (Composite 2, Fig. 10 (b)), while C can be as large as 0.5 for the composite containing the less wear-resistant reinforcement for the wear rate to exceed the upper bound. That is, a composite with a more wear-resistant reinforcement can tolerate a lower level of toughness than a composite containing a less wear-resistant reinforcement. This result is consistent with experimental observations made by other investigators [1,8-12], and indicates that the proposed coefficient C has a strong physical basis for the class of hard reinforcement composites considered here.

B. Experimental results

The results of the pin-on-drum two-body abrasive wear tests are shown in Figs. 11 and 12. The interfacial toughness and the relative size of the reinforcement were changed to effect a variation in the contribution coefficient C . Test results for the composites with

different interfacial conditions, in the form of “strong” and “weak” interfaces, are displayed in Fig. 11.

For both composites, the experimental results are in reasonable agreement with the model predictions using a value for the contribution coefficient of $C = 0.4$ for the “strong interface” composite, and $C = 0$ for the “weak interface” material. Such predictions are consistent with observations that poor interfacial toughness induces large interfacial crack sizes corresponding to a low contribution by the reinforcement.

Since the relative size of the reinforcement is small in particulate-reinforced composites, the effect of the interfacial toughness on the wear rate can be significant. For example, when the interface is weak, the reinforcement can be readily removed during abrasive wear conditions, such that a negative reinforcement effect is observed. Indeed, as shown in Fig. 11 (b), the wear rates in the composite were higher than those in the unreinforced matrix; moreover, with increasing reinforcement volume fraction, the wear rates were further increased.

The abrasive wear rates of composites with different relative sizes of the reinforcement (relative to the abrasive medium) are plotted in Fig. 12. It can be seen that for the case of a large reinforcement particle size relative to abrasive size, which corresponds to classical abrasive wear conditions, a value of $C = 0.4$ shows good agreement with the experimental results (Fig. 12 (a)). The experimental data fall within the rules of mixtures bounds, exceeding the upper bound at a reinforcement volume fraction of about 0.5. When the reinforcement particle is small relative to the abrasive size, however, the wear rates increase considerably for the same composite material (Fig. 12 (b)). This is due to plowing by the abrasive medium, leading to a higher wear rate associated with debonding and particle removal mechanisms. This physically-based consideration is not in the rules of mixtures formulations. Once again, test results are consistent with the current model’s predictions.

CONCLUSIONS

A simple framework for a physically based model for abrasive wear in ductile composites reinforced with a hard second phase is presented based on the salient mechanisms of sliding wear, namely plowing, cracking at the matrix/reinforcement interface or in the reinforcement, and particle removal. The model relies on the straightforward notion that any portion of reinforcement that is removed as wear debris cannot contribute to the wear resistance of the material; the size of this non-contributing portion (NCP) of the reinforcement is estimated from the mechanistic descriptions. The model provides a rationale for the contribution coefficient, C . The limitations inherent in such a model are that it does not take into account additional mechanisms possible in a three-dimensional model, such as torsional and out-of-plane particle removal modes. However, since the abrasive wear data were obtained from pin-on-drum tests where the wear path is essentially linear, one would expect that the predominant wear mechanisms to lie along the two-dimensional plane represented by the proposed model. While the

torsional and out-of-plane particle pull-out mechanisms are certainly likely, this contributions to the overall wear rate are expected to be secondary. Critical variables describing the role of the reinforcement are identified in terms of the relative size of the reinforcement, the depth of plowing and the toughness of the matrix/reinforcement interface or the reinforcement. The model provides a reasonable description of the variation in abrasive wear rates with reinforcement volume fraction and provides a justification for the “negative reinforcement” effect.

ACKNOWLEDGMENTS

Support for one of the authors (ROR) was provided by the Director, Office of Science, Office of Basic Energy Sciences, Materials Sciences Division of the U.S. Department of Energy under Contract No. DE-AC03-76SF00098.

REFERENCES

1. K.J. Bhansali and R. Mehrabian, Abrasive wear of aluminum-matrix composites, *Journal of Metals*, 34 (1982) 30-34.
2. C.P. Dogan and J.A. Hawk, Role of zirconia toughening in the abrasive wear of intermetallic and ceramic composites, *Wear*, 212 (1997) 110-118.
3. D.Holz, R. Janssen, K. Friedrich and N. Claussen, Abrasive wear of ceramic-matrix composites, *Journal of the European Ceramic Society*, 5 (1989) 229-232.
4. M.M. Khrushov, Principles of abrasive wear, *Wear*, 28 (1974) 69-88.
5. S. Skoliannos and T.Z. Kattamis, Tribological properties of SiC/sub p/-reinforced Al-4.5% Cu-1.5% Mg alloy composites, *Materials Science & Engineering A (Structural Materials: Properties, Microstructure and Processing)*, 163 (1993) 107-113.
6. K.H. Zum-Gahr, Abrasive wear of two-phase metallic materials with a coarse microstructure, in: K.C. Ludema (ed.), *International Conference on Wear of Materials*, American Society of Material Engineering, Vancouver, 1985, 793 p.
7. M.M. Khrushov and M.A. Babichev, Resistance to abrasive wear of structurally heterogeneous materials, *Friction and Wear in Machinery*, 12 (1958) 5-24.
8. N. Axen and S. Jacobson, A model for the abrasive wear resistance of multiphase materials, *Wear*, 174 (1994) 187-199.
9. B. Yen and C. K. H. Dharan, A model for the abrasive wear of fiber-reinforced polymer composites, *Wear*, 195 (1996) 123-127.
10. N. Axen and K.H. Zum-Gahr, Abrasive wear of TiC-steel composite clad layers on tool steel, *Wear*, 157 (1992) 189-201.
11. N. Axen, A. Alahelisten, and S. Jacobson, Abrasive wear of alumina fibre-reinforced aluminium, *Wear*, 173 (1994) 95-104.
12. N. Axen and S. Jacobson, Transitions in the abrasive wear resistance of fibre- and particle- reinforced aluminium, *Wear*, 178 (1994) 1-7.
13. F.M. Hosking, F. Folgar Portillo, R. Wunderlin and R. Mehrabian, Composites of aluminium alloys: fabrication and wear behaviour, *Journal of Materials Science*, 17 (1982) 477-498.
14. S.V. Prasad and P.D. Calvert, Abrasive wear of particle-filled polymers, *Journal of Materials Science*, 15 (1980) 1746-1754.
15. S.-J. Liu, and K.-S. Lin, Effect of aging on abrasion rate in an Al-Zn-Mg-SiC composite, *Wear*, 121 (1988) 1-14.
16. S.V. Prasad and P.K. Rohatgi, Tribological properties of Al alloy particle composites, *Journal of Metals*, 39 (1987) 22-26.
17. W. Simm and S. Freti, Abrasive wear of multiphase materials, *Wear*, 129 (1989) 105-121.
18. A.C.M. Yang, J.E. Ayala, A. Bell and J.C. Scott, Effects of filler particles on abrasive wear of elastomer-based composites, *Wear*, 146 (1991) 349-366.
19. Z.F. Zhang, L.C. Zhang, and Y.W. Mai, Wear of ceramic particle-reinforced metal-matrix composites. I. Wear mechanisms, *Journal of Materials Science*, 30 (1995) 1961-1966.
20. Z.F. Zhang, L.C. Zhang, and Y.W. Mai, Particle effects on friction and wear of aluminum matrix composites, *Journal of Materials Science*, 30 (1995) 5999-6004.

21. B.K. Prasad, *et al.*, Abrasive wear characteristics of Zn-37.2Al-2.5Cu-0.2Mg alloy dispersed with silicon carbide particles, *Materials Transactions*, 36 (1995) 1048-1057.
22. I.M. Hutchings, *Tribology; Friction and wear of engineering materials*, Arnold, London, 1992, 273 p.
23. K.-H. Zum-Gahr, *Microstructure and wear of materials*. Tribology Series 10, Elsevier Science, New York, 1987, 560 p.
24. W.M. Garrison, Khrushov's rule and the abrasive wear resistance of multiphase solids, *Wear*, 82 (1982) 213-220.
25. S.R. White and R.G. Albers, Experimental investigation of aluminum/epoxy interfacial properties in shear and tension, *Journal of Adhesion*, 55 (1996) 303-316.
26. M.-Y. He and J.W. Hutchinson, Crack deflection at an interface between dissimilar elastic materials, *International Journal of Solids Structures*, 25 (1989) 1053-1067.
27. *Annual Book of ASTM Standards*, American Society for Metals, West Conshohocken, PA, 1999, 544 p.

FIGURE CAPTIONS

- Fig. 1. Predicted abrasive wear rates of composites. Eqs. (1) and (2) represent the lower and upper limits of the existing methods. Experimental results (region A) of composites reinforced with hard particles often lie outside these bounds [1,10-14].
- Fig. 2. General schematic drawing of a two-phase composite in abrasion with simplified geometry in two-dimensions: a triangular abrasive medium and rectangular reinforcements.
- Fig. 3. Abrasive particles plow the matrix and reinforcement alternatively forming stress fields around them; compressive stresses are created in front and tensile stresses behind the abrasive particle.
- Fig. 4. With a “weak” interface between the matrix and the reinforcement, the motion of abrasive medium leads the crack propagation along the interface (a). When the matrix/reinforcement interface is relatively “strong” in that the ratio of the fracture toughness between interface and reinforcement is larger than ~ 0.25 for this geometry, the crack penetrates into the reinforcement (b) [26].
- Fig. 5. (a) The tip of the interfacial crack reaches the bottom of the reinforcing particle and continues to propagate around the particle. (b) The size of the non-contributing portion (NCP) of reinforcement due to the failure at the matrix/reinforcement interface is $(x + a_{int})$.
- Fig. 6. (a) When the tip of the crack reaches the reinforcement/matrix interface, continuous motion of abrasive medium causes removal of a portion of the reinforcement as a large mass. (b) The size of the non-contributing portion (NCP) of the reinforcement per path of each abrasive medium is $(a_R \times x)/\text{path}$.
- Fig. 7. Scanning electron micrograph of aluminum particulate-reinforced epoxy composite with 40 vol.% of the reinforcement. The average size of the reinforcing particles is $\sim 100 \mu\text{m}$.
- Fig. 8. Scanning electron micrographs of alumina abrasive: (a) coarse abrasive with an average size of $326 \mu\text{m}$ (p50 grit), (b) with an average size of $127 \mu\text{m}$ (p120 grit), and (c) fine abrasive with an average size of $35 \mu\text{m}$ (p400 grit).
- Fig. 9. Pin-on-drum abrasive wear test set-up. The drum is 150 mm in diameter and rotates at 25 rpm resulting in a tangential velocity of 0.2 m/s. The longitudinal traverse is 4.2 mm/rev of the drum. A counter records the number of revolutions. The composite specimen is loaded onto the drum with a specified weight.
- Fig. 10. Prediction of abrasive wear rates, normalized to the wear rate of the reinforcement, for two ideal composites with different contribution coefficients and volume fractions. The two composites, termed composite 1 and 2, differ in

their relative wear resistance; the abrasive wear resistance of the reinforcement in composite 2 is twice as large as that of the reinforcement in composite 1. Plots are for various values of the contribution coefficient, C . The shaded region represents the predictions from the rule of mixtures models, Eqs. (1) and (2).

Fig. 11. Abrasive wear rates of particulate reinforced model composites with different interfacial properties between matrix and reinforcement, showing predictions for (a) a strong interface ($a_{\text{int}} \ll D_R$), and (b) a very weak interface ($a_{\text{int}} \sim D_R$). The line through the experimental results for Al-reinforced epoxy matrix composites is shown as a solid line; predictions are dashed lines. The shaded region represents the predictions from the rule of mixtures models, Eqs. (1) and (2).

Fig. 12. Abrasive wear rates with different relative size of the reinforcement relative to the abrasive medium, showing experimental results for Al-reinforced epoxy composites (solid lines with data points) and model predictions (dashed lines) for composites with a) large reinforcement size ($D_R > x$), and b) small reinforcement size ($D_R \sim x$). The shaded region represents the predictions from the rule of mixtures models, specifically Eqs. (1) and (2).

Table 1: Surface roughness of the neat matrix tested with different sizes of abrasive and at the same applied normal load of 2.94 N (corresponding to a stress of 41.3 kPa).

Alumina abrasive size	Root mean square roughness, R_q (μm)	Peak-to-valley dimension, V_{max} (μm)
35 μm (p400 grit)	2.3	5
127 μm (p120 grit)	10.5	50
326 μm (p50 grit)	21.5	90

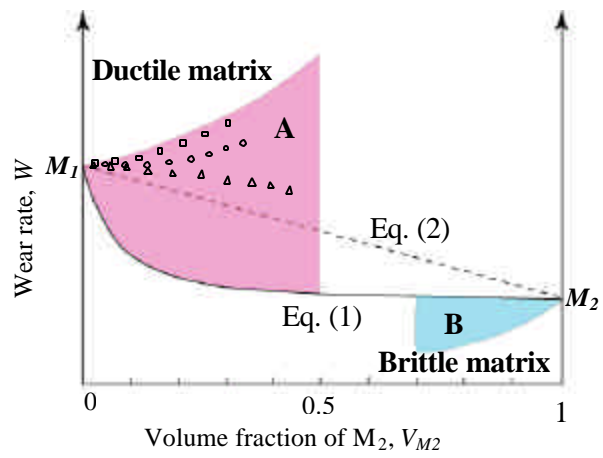


Fig. 1. Predicted abrasive wear rates of composites. Eqs. (1) and (2) represent the lower and upper limits of the existing methods. Experimental results (region A) of composites reinforced with hard particles often lie outside these bounds [1,10-14].

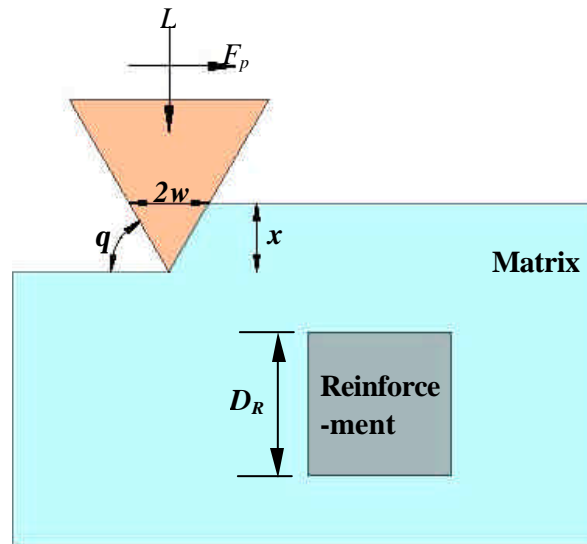


Fig. 2. General schematic drawing of a two-phase composite in abrasion with simplified geometry in two-dimensions: a triangular abrasive medium and rectangular reinforcements.

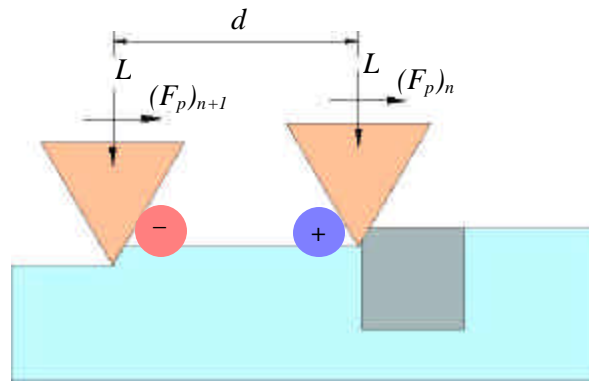
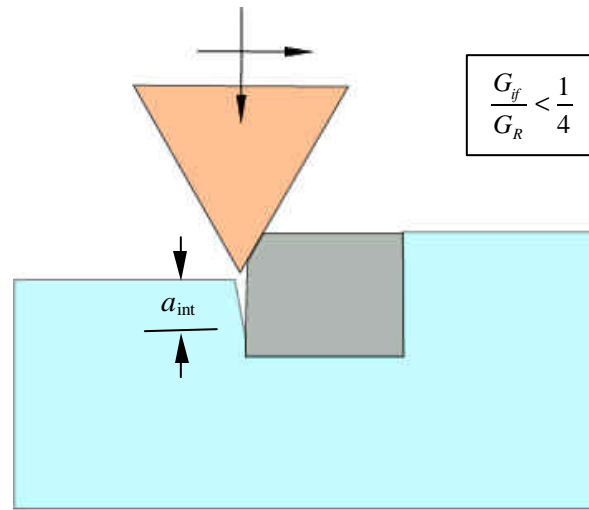
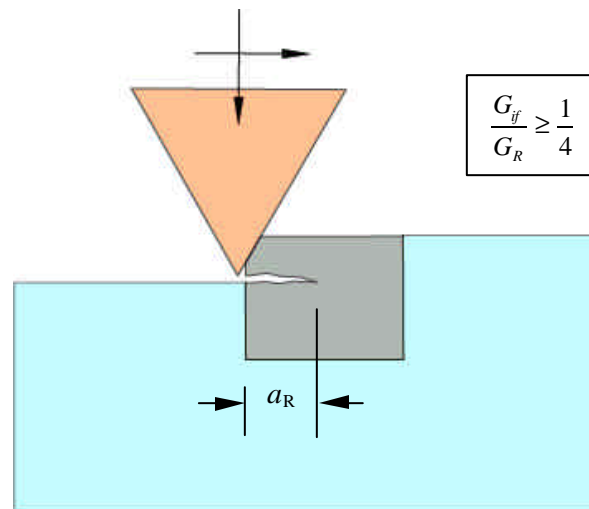


Fig. 3. Abrasive particles plow the matrix and reinforcement alternatively forming stress fields around them; compressive stresses are created in front and tensile stresses behind the abrasive particle.

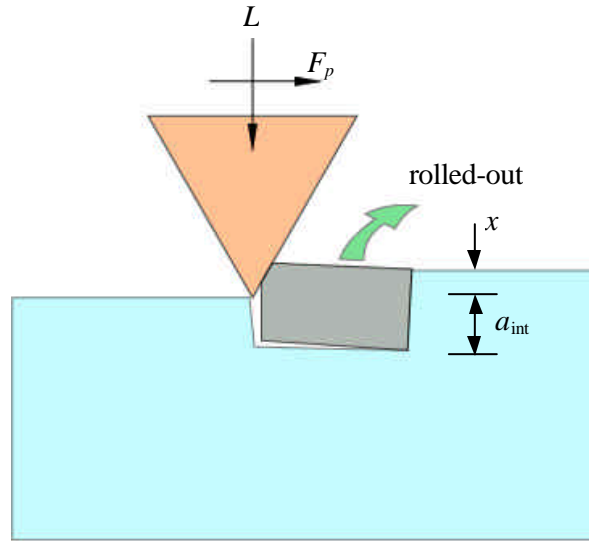


(a)

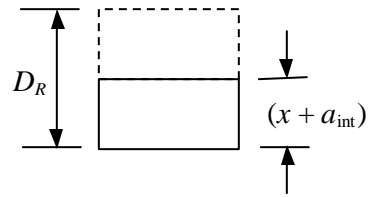


(b)

Fig. 4. With a “weak” interface between the matrix and the reinforcement, the motion of abrasive medium leads the crack propagation along the interface (a). When the matrix/reinforcement interface is relatively “strong” in that the ratio of the fracture toughness between interface and reinforcement is larger than ~ 0.25 for this geometry, the crack penetrates into the reinforcement (b) [26].



(a)



(b)

Fig. 5. (a) The tip of the interfacial crack reaches the bottom of the reinforcing particle and continues to propagate around the particle. (b) The size of the non-contributing portion (NCP) of reinforcement due to the failure at the matrix/reinforcement interface is $(x + a_{\text{int}})$.

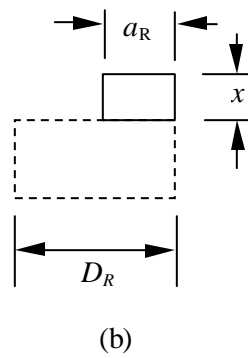
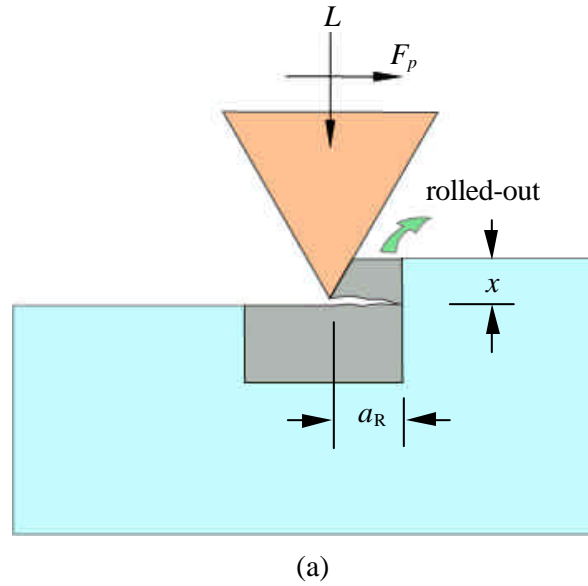


Fig. 6.(a) When the tip of the crack reaches the reinforcement/matrix interface, continuous motion of abrasive medium causes removal of a portion of the reinforcement as a large mass. (b) The size of the non-contributing portion (NCP) of the reinforcement per path of each abrasive medium is $(a_R \times x)/\text{path}$.

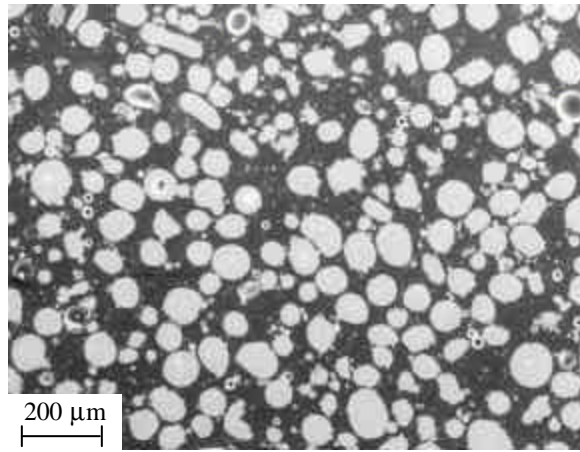


Fig. 7. Scanning electron micrograph of aluminum particulate-reinforced epoxy composite with 40 vol.% of the reinforcement. The average size of the reinforcing particles is $\sim 100 \mu\text{m}$.

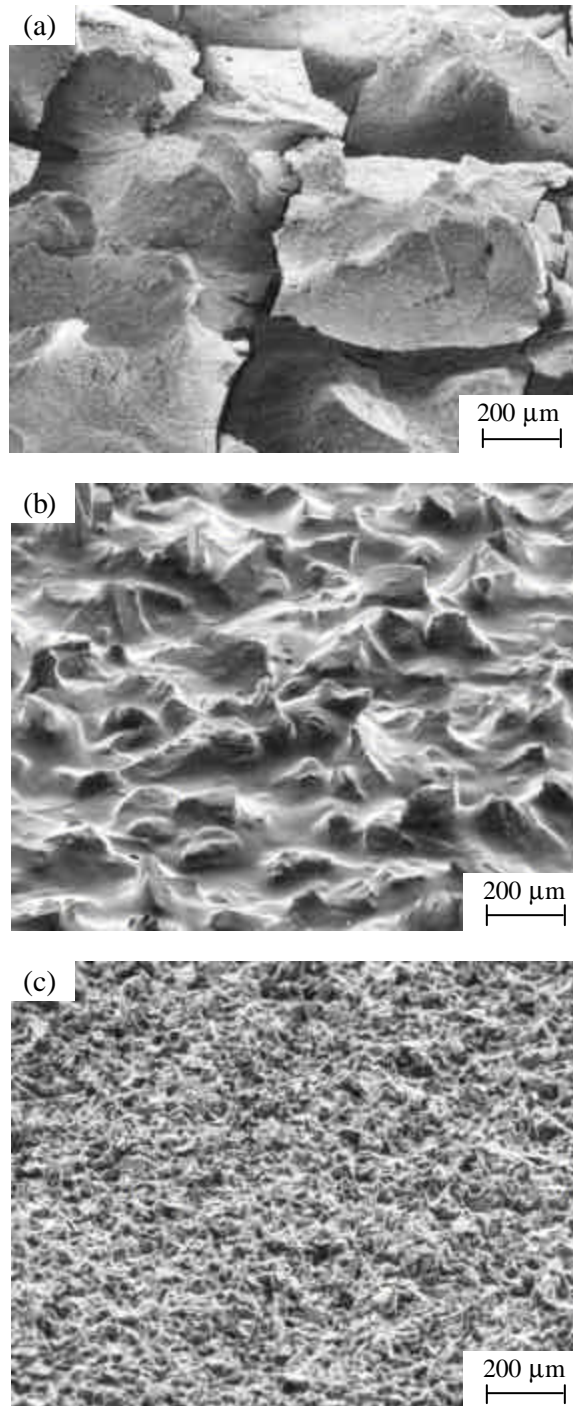


Fig. 8. Scanning electron micrographs of alumina abrasive: (a) coarse abrasive with an average size of 326 μm (p50 grit), (b) with an average size of 127 μm (p120 grit), and (c) fine abrasive with an average size of 35 μm (p400 grit).

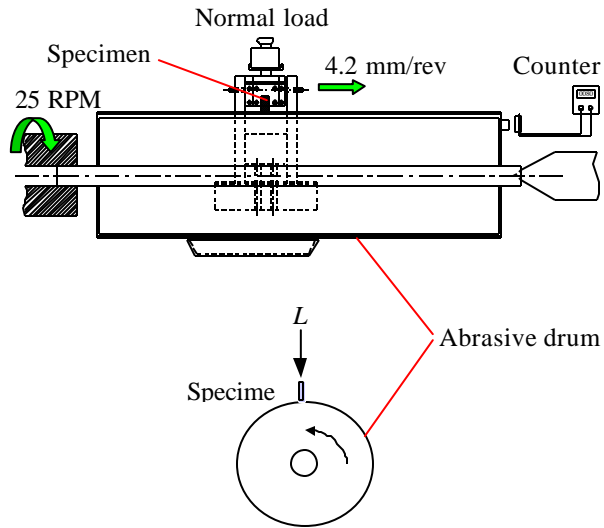
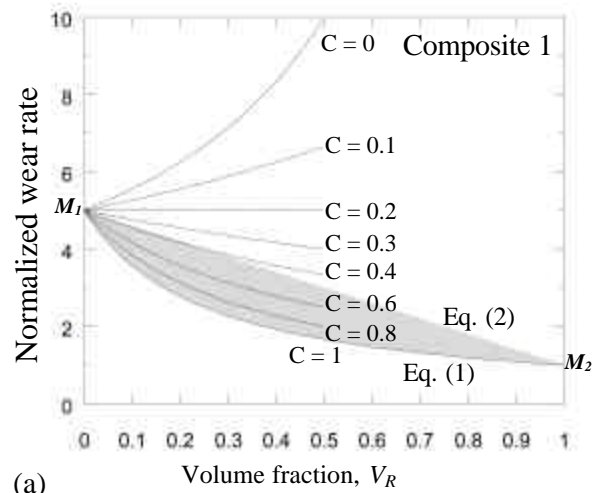


Fig. 9. Pin-on-drum abrasive wear test set-up. The drum is 150 mm in diameter and rotates at 25 rpm resulting in a tangential velocity of 0.2 m/s. The longitudinal traverse is 4.2 mm/rev of the drum. A counter records the number of revolutions. The composite specimen is loaded onto the drum with a specified weight.



$$\frac{W_{M2}}{W_{M3}} = \frac{2}{1}$$

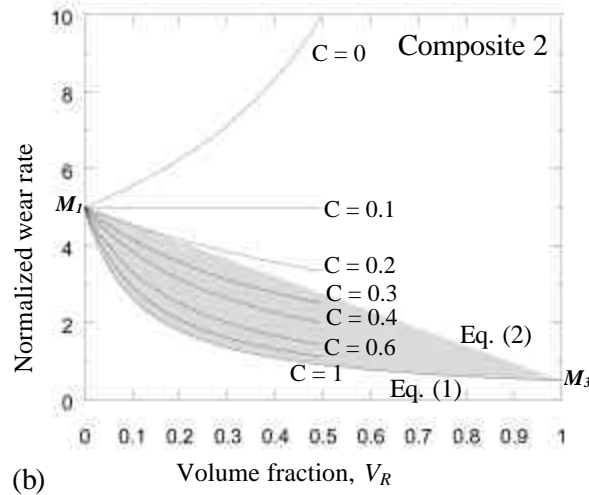
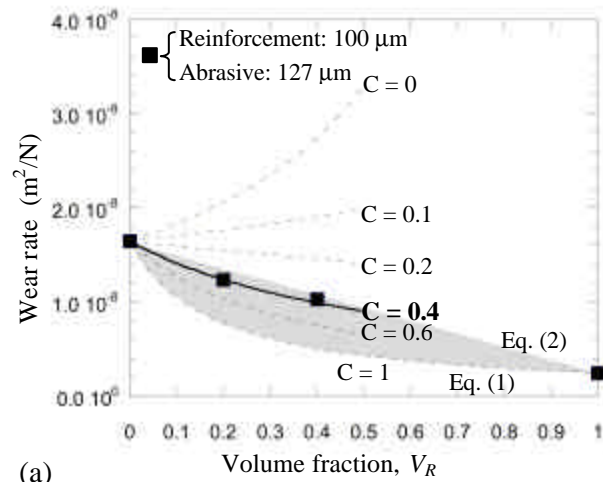
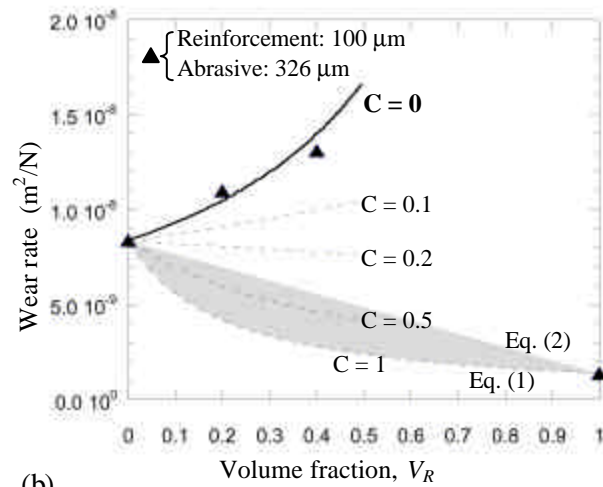


Fig. 10. Prediction of abrasive wear rates, normalized to the wear rate of the reinforcement, for two ideal composites with different contribution coefficients and volume fractions. The two composites, termed composite 1 and 2, differ in their relative wear resistance; the abrasive wear resistance of the reinforcement in composite 2 is twice as large as that of the reinforcement in composite 1. Plots are for various values of the contribution coefficient, C . The shaded region represents the predictions from the rule of mixtures models, Eqs. (1) and (2).



(a)



(b)

Fig. 11. Abrasive wear rates of particulate reinforced model composites with different interfacial properties between matrix and reinforcement, showing predictions for (a) a strong interface ($a_{\text{int}} \ll D_R$), and (b) a very weak interface ($a_{\text{int}} \sim D_R$). The line through the experimental results for Al-reinforced epoxy matrix composites is shown as a solid line; predictions are dashed lines. The shaded region represents the predictions from the rule of mixtures models, Eqs. (1) and (2).

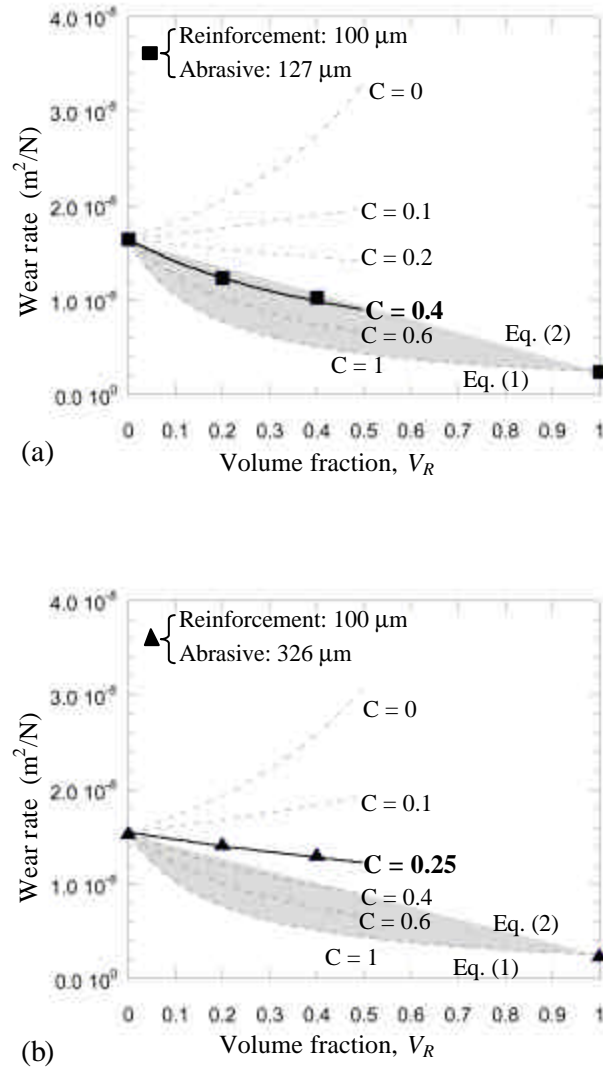


Fig. 12. Abrasive wear rates with different relative size of the reinforcement relative to the abrasive medium, showing experimental results for Al-reinforced epoxy composites (solid lines with data points) and model predictions (dashed lines) for composites with a) large reinforcement size ($D_R > x$), and b) small reinforcement size ($D_R \sim x$). The shaded region represents the predictions from the rule of mixtures models, specifically Eqs. (1) and (2).